H1prelim-08-161 Submitted to

34th International Conference on High Energy Physics, ICHEP2008, 30th July - 5th August, Philadelphia
Abstract: **873**
Parallel Session **EXOTIC II: leptoquarks, compositeness**

Electronic Access:https://www-h1.desy.de/publications/H1preliminary.short_list.html

Search for Excited Quarks in ep Collisions at HERA

H1 Collaboration

Abstract

A search for excited quarks is performed using the full $e^{\pm}p$ data sample collected by the H1 experiment at HERA, corresponding to a total luminosity of 475 pb^{-1}. The electroweak decays of excited quarks $q^* \rightarrow q\gamma$, $q^* \rightarrow qZ$ and $q^*\rightarrow qW$ with subsequent hadronic or leptonic decays of the W and Z bosons are considered. No evidence for excited quark production is found. Mass dependent exclusion limits on the ratio f/Λ of the coupling to the compositeness scale are derived within gauge mediated models. These limits extend the excluded region compared to previous excited quark searches.

1 Introduction

The three-family structure and mass hierarchy of the known fermions is one of the most puzzling characteristics of the Standard Model (SM) of particle physics. Attractive explanations are provided by models assuming composite quarks and leptons [1]. The existence of excited states of leptons and quarks is a natural consequence of these models and their discovery would provide convincing evidence of a new scale of matter. Electron[1]-proton interactions at very high energies provide good conditions to look for excited states of first generation fermions.

In this paper a search for excited quarks using the complete $e^{\pm}p$ HERA collider data of the H1 experiment is presented. Electroweak decays into a SM quark and a SM gauge boson (γ, W and Z) are considered and hadronic as well as leptonic decays of the W and Z are analysed.

The data are recorded at electron beam energy of 27.6 GeV and proton beam energies of 820 GeV and 920 GeV, corresponding to centre-of-mass energies $\sqrt{s}$ of 301 GeV and 319 GeV, respectively. The total integrated luminosity of the data is 475 pb^{-1}. The data comprise 184 pb^{-1} recorded in e^-p collisions and 291 pb^{-1} in e^+p collisions, of which 35 pb^{-1} were recorded at $\sqrt{s} = 301$ GeV. With more than a twelve-fold increase in statistics and an higher centre-of-mass energy, this analysis supersedes the result of the previous H1 search for excited quarks [2]. It complements the search for first generation excited neutrinos [3] and electrons [4].

2 Phenomenology

In the present study a model [5–7] is considered in which excited fermions are assumed to have spin $1/2$ and isospin $1/2$. The left-handed and right-handed components of the excited fermions form weak iso-doublets F_L^* and F_R^*.

Interactions between excited and ordinary fermions may be mediated by gauge bosons, as described by the effective Lagrangian [6, 7]:

$$\mathcal{L}_{int.} = \frac{1}{2\Lambda}\bar{F}_R^* \, \sigma^{\mu\nu} \left[g f \frac{\tau^a}{2} W_{\mu\nu}^a + g' f' \frac{Y}{2} B_{\mu\nu} + g_s f_s \frac{\lambda^a}{2} G_{\mu\nu}^a \right] \; F_L + h.c. \; . \tag{1}$$

Only the right-handed component of the excited fermions F_R^* is allowed to couple to light fermions, in order to protect the light leptons from radiatively acquiring a large anomalous magnetic moment [8, 9]. The matrix $\sigma^{\mu\nu}$ is the covariant bilinear tensor, $W_{\mu\nu}^a$, $B_{\mu\nu}$ and $G_{\mu\nu}^a$ are the field-strength tensors of the SU(2), U(1) and SU(3)$_C$ gauge fields, τ^a, Y and λ^a are the Pauli matrices, the weak hypercharge operator and the Gell-Mann matrices, respectively. The standard electroweak and strong gauge couplings are denoted by g, g' and g_s, respectively. The parameter Λ has units of energy and can be regarded as the compositeness scale which reflects the range of the new confinement force. The constants f, f' and f_s are coupling parameters associated to the three gauge groups and are determined by the yet unknown composite dynamics.

Following this model of gauge mediated interactions, excited quarks may be resonantly produced in ep collisions through a t-channel gauge boson exchange between the incoming

[1] In this paper "electron" refers to both electron and positrons, if not otherwise stated.

electron and a quark of the proton. Excited quarks may also be exchanged in the u-channel with a non negligible cross section for high q^* masses and low values of Λ. Only electroweak couplings of the q^* will be considered in the present study and $f_s = 0$ will be assumed. This assumption allows to make a complementary study to q^* searches performed at the Tevatron as at a $p\bar{p}$ collider excited quarks are produced in a quark-gluon fusion mechanism which requires $f_s \neq 0$. If $f_s = 0$, the excited quark may decay into a quark and an electroweak gauge boson via $q^* \to q\gamma$, $q^* \to qW$ and $q^* \to qZ$. For a given q^* mass value (M_{q^*}) and assuming a numerical relation between f and f', the q^* branching ratios are fixed and the production cross section depends only on f/Λ. The assumption is made that the coupling parameters f and f' are of comparable strength and only the relationship $f = +f'$ is considered.

3 Simulation of Signal and Background Processes

The Monte Carlo (MC) program H1QSTAR developed for this analysis is used for the calculation of the $q^* \to q\gamma$ production cross section and the simulation of signal events in this channel. The cross section is calculated from the Lagrangian described in equation (1) using the CompHEP package [10]. Both resonant $q*$ production and u-channel exchange processes and their interference are included. The MC event generator COMPOS [11] is used for the simulation of signal events in the $q^* \to qW$ and $q^* \to qZ$ channels and for the calculation of the corresponding cross section. In both event generators initial state radiation of a photon from the incident electron is included using the Weizsäker-Williams approximation [12]. The proton parton densities are taken from the CTEQ5L [13] parametrisation. The parton shower approach [14] is applied in order to simulate Quantum Chromodynamics (QCD) corrections in the initial and final states. Hadronisation is performed using Lund string fragmentation as implemented in PYTHIA [14].

The COMPOS generator uses the narrow width approximation (NWA) for the calculation of the production cross section and takes into account the natural width of the excited quark for the q^* decay. The NWA is valid for q^* masses below 290 GeV and the couplings f/Λ relevant to this analysis, as the total q^* width is less than 10% of the q^* mass. In the H1QSTAR generator the full transition matrix including the production and the decay is implemented. Events used in the determination of signal efficiencies are generated with the coupling f/Λ corresponding, for each q^* mass, to the expected boundary of the probed domain in the plane defined by M_{q^*} and f/Λ.

The Standard Model (SM) processes which may mimic the q^* signal are prompt photon production, neutral current (NC) deep-inelastic scattering (DIS) events, photoproduction and to a lesser extent real W boson production and lepton pair production.

The RAPGAP [15] event generator, which implements the Born, QCD Compton and Boson Gluon Fusion matrix elements, is used to model NC DIS events. The QED radiative effects arising from real photon emission from both the incoming and outgoing electrons are simulated using the HERACLES [16] program. Direct and resolved photoproduction of jets and prompt photon production are simulated using the PYTHIA event generator. The simulation is based on Born level hard scattering matrix elements with radiative QED corrections. In RAPGAP and PYTHIA, jet production from higher order QCD radiation is simulated using leading logarithmic parton showers and hadronisation is modelled with Lund string fragmentation. The leading order MC prediction of NC DIS and photoproduction processes with two or more high transverse momentum jets is scaled by a factor of 1.2 to account for missing higher orders in the MC generators [19,20]. Charged current DIS events are simulated using the DJANGO [17] program, which includes first order leptonic QED radiative corrections based on HERACLES. The production of two or more jets in DJANGO is accounted for using the colour-dipole-model [18]. Contributions from elastic and quasi-elastic QED Compton scattering are simulated with the WABGEN [21] generator. Contributions arising from the production of W bosons and multi-lepton events are modelled using the EPVEC [22] and GRAPE [23] event generators, respectively.

All processes are generated with at least 10 times the integrated luminosity of the data sample. Generated events are passed through the full GEANT [24] based simulation of the H1 apparatus, which takes into account the actual running conditions of the data taking, and are reconstructed and analysed using the same program chain as for the data.

4 Experimental Conditions

A detailed description of the H1 experiment can be found in [25]. Only the detector components relevant to the present analysis are briefly described here. The origin of the H1 coordinate system is the nominal ep interaction point, with the direction of the proton beam defining the positive z-axis (forward region). Transverse momentum (P_T) is measured in the xy plane. The pseudorapidity η is related to the polar angle θ by $\eta = -\ln\,\tan(\theta/2)$. The Liquid Argon (LAr) calorimeter [26] is used to measure electrons, photons and hadrons. It covers the polar angle range $4^\circ < \theta < 154^\circ$ with full azimuthal acceptance. Electromagnetic shower energies are measured with a precision of $\sigma(E)/E = 12\%/\sqrt{E/\text{GeV}} \oplus 1\%$ and hadronic energies with $\sigma(E)/E = 50\%/\sqrt{E/\text{GeV}} \oplus 2\%$, as measured in test beams [27, 28]. In the backward region, energy measurements are provided by a lead/scintillating-fiber (SpaCal) calorimeter [29] covering the angular range $155^\circ < \theta < 178^\circ$. The central ($20^\circ < \theta < 160^\circ$) and forward ($7^\circ < \theta < 25^\circ$) tracking detectors are used to measure charged particle trajectories, to reconstruct the interaction vertex and to complement the measurement of hadronic energy. The innermost proportional chamber CIP ($9^\circ < \theta < 171^\circ$) is used to veto charged particles for the identification of photons. The LAr calorimeter and inner tracking detectors are enclosed in a super-conducting magnetic coil with a field strength of 1.16 T. From the curvature of charged particle trajectories in the magnetic field, the central tracking system provides transverse momentum measurements with a resolution of $\sigma_{P_T}/P_T = 0.005 P_T/\text{GeV} \oplus 0.015$ [30]. The return yoke of the coil is the outermost part of the detector and is equipped with streamer tubes forming the central muon detector ($4^\circ < \theta < 171^\circ$). In the forward region of the detector ($3^\circ < \theta < 17^\circ$) a set of drift chambers detects muons and measures their momenta using an iron toroidal magnet. The luminosity is determined from the rate of the Bethe-Heitler process $ep \rightarrow ep\gamma$, measured using a photon detector located close to the beam pipe at $z = -103$ m, in the backward direction.

5 Data Analysis

The triggers employed for collecting the data used in this analysis are based on the detection of electromagnetic deposits or missing transverse energy in the LAr calorimeter [31]. For events with missing transverse energy of 20 GeV, the trigger efficiency is $\sim 90\%$ and increases above 95% for missing transverse energy above 30 GeV. Events containing an electromagnetic deposit (electron or photon) with an energy greater than 10 GeV are triggered with an efficiency close to 100%. Events triggered only by jets have a trigger efficiency of nearly 100% for $P_T^{\rm jet} > 20$ GeV.

In order to remove background events induced by cosmic showers and other non-ep sources, the event vertex is required to be reconstructed within 35 cm in z of the nominal interaction point. In addition, topological filters and timing vetoes are applied.

The identification of electrons or photons relies on the measurement of a compact and isolated electromagnetic shower in the LAr calorimeter. In addition, the hadronic energy within a distance in the pseudorapidity-azimuth $(\eta - \phi)$ plane $R = \sqrt{\Delta\eta^2 + \Delta\phi^2} < 0.5$ around the electron (photon) is required to be below 3% of the electron (photon) energy. Furthermore, each electron (photon) candidate must be isolated from jets by a minimum distance in pseudorapidity-azimuth of $R > 0.5$ to any jet axis. The electron and photon energy and angular direction are measured by the calorimeters. Muon identification is based on a track measured in the inner tracking systems associated with signals in the muon detectors [32, 33]. A muon candidate should have no more than 5 GeV deposited in a cylinder, centred on the muon track direction, of radius 25 cm and 50 cm in the electromagnetic and hadronic sections of the LAr calorimeter, respectively. Additionally, the muon candidate is required to be separated from the closest jet and from any track by $R > 1$ and $R > 0.5$, respectively. Calorimeter energy deposits and tracks not previously identified as electron, photon or muon candidates are used to form combined cluster-track objects, from which the hadronic energy is reconstructed [34, 35]. Jets are reconstructed from these combined cluster-track objects using an inclusive k_T algorithm [36, 37] with a minimum transverse momentum of 2.5 GeV. The missing transverse momentum $P_T^{\rm miss}$ of the event is derived from all detected particles and energy deposits in the event. In events with large $P_T^{\rm miss}$, the only non-detected particle in the event is assumed to be a neutrino. The four-vector of this neutrino candidate is reconstructed assuming transverse momentum conservation and the relation $\sum_i (E^i - P_z^i) + (E^\nu - P_z^\nu) = 2E_e^0 = 55.2$ GeV, where the sum runs over all detected particles; P_z is the momentum along the proton beam axis and E_e^0 is the electron beam energy.

Specific selection criteria applied in each decay channel are presented in the following subsections.

5.1 $q\gamma$ Resonance Search

The signature of the $q^* \to q\gamma$ decay channel consists of one high P_T isolated electromagnetic cluster and one high P_T jet. SM background arises from NC DIS and prompt photon events. Events are selected with a photon candidate with transverse momentum $P_T^\gamma > 35$ GeV in a polar angle range $5° < \theta^\gamma < 90°$. The events are required to have at least one jet in the polar angle range $5° < \theta^{\rm jet} < 90°$ with a transverse momentum larger than 20 GeV. In the central region

($\theta^\gamma > 20°$), photon candidates are selected only if no track points to the electromagnetic cluster within a distance of closest approach (DCA) of 30 cm or within $R < 0.5$. In the forward region ($\theta^\gamma < 20°$) only photon candidates having no well measured track with a DCA to the cluster below 12 cm are accepted. In this region, the calorimetric isolation of the photon candidate is also tigthened by requiring that the hadronic energy within $R < 1$ around the photon be below 3% of the photon energy. In addition, it is required that no hit in the CIP be associated to the photon candidate. Photoproduction backgrounds typically have low values of the Bjorken scaling variable, x_h, calculated from the hadronic system using the Jacquet-Blondel method [38, 39], and are thus reduced by requiring $x_h > 0.1$. Finally, to further reduce the background from NC DIS, it is required that no electromagnetic deposit with an energy larger than 10 GeV and with a track associated to it be present in the LAr.

After this selection, 47 events are found in the data compared to an expected SM contribution of 47 ± 7 events. The errors on the SM prediction includes model and experimental systematic errors added in quadrature (see section 5.5). The invariant mass of the q^* candidate is calculated from the four-vectors of the photon and highest P_T jet candidates. The invariant mass distribution of the q^* candidates and the SM background expectations is presented in figure 1(a). The selection efficiency is 35% for $M_{q^*} = 120$ GeV, increasing to 45% for $M_{q^*} = 260$ GeV. From Monte Carlo studies, the experimental resolution on the reconstructed q^* mass distribution is 6 GeV for a generated q^* mass of 120 GeV, increasing to 12 GeV for an q^* mass of 260 GeV.

5.2 $qq\bar{q}$ Resonance Search

The signature of the $q^* \to qW \to qq\bar{q}$ and $q^* \to qZ \to qq\bar{q}$ decay channels is similar and consists of three high transverse momentum jets. The SM background is dominated by multi-jet photoproduction and NC DIS events. Events are selected with at least three jets in the polar angle range $5° < \theta^{\mathrm{jet}} < 120°$ with transverse momenta larger than 50, 30 and 15 GeV, respectively. In each event, a W or Z boson candidate is reconstructed from the combination of the two jets among all jets present in the event having an invariant mass closest to the nominal W or Z boson mass. The reconstructed mass of the W or Z candidate is required to be larger than 70 GeV and smaller than 100 GeV. Furthermore, in decays of q^* of large mass, the highest P_T jet often does not originate from the boson decay. Therefore, only events in which the highest P_T jet is not associated to the W or Z boson candidate are selected. This strongly reduces the photoproduction background.

After this selection, 346 events are observed while 338 ± 137 are expected from the SM. The invariant mass of the q^* candidate is calculated from the highest P_T jet and W or Z candidate four-vectors. The invariant mass distribution of the q^* candidates and of the SM background is presented in figure 1(b). The selection efficiency in this channel is 5% for $M_{q^*} = 120$ GeV, increasing to 60% for $M_{q^*} = 260$ GeV. From Monte Carlo studies, the experimental resolution on the reconstructed q^* mass distribution is 8 GeV for a generated q^* mass of 120 GeV, increasing to 14 GeV for a q^* mass of 260 GeV.

5.3 $qe\nu$ and $q\mu\nu$ Resonance Searches

In the search for $q^* \to qW \to qe\nu$, events with $P_T^{\mathrm{miss}} > 25$ GeV, one electron with $P_T^e > 10$ GeV and one jet with $P_T^{\mathrm{jet}} > 20$ GeV are selected. The electron and the jet must be detected in the polar angle range $5^\circ < \theta < 100^\circ$. Furthermore, the electron must be isolated from jets by a minimum distance of $R > 1$ and in the polar angle region $\theta^e > 35^\circ$ the electron must be associated to a charged track. The ratio V_{ap}/V_p of transverse energy flow anti-parallel and parallel to the hadronic final state [38] is used to suppress photoproduction and NC DIS events. Events with $V_{ap}/V_p > 0.25$ are rejected. The invariant mass of the W boson candidate, reconstructed from the four-vectors of the electron and neutrino candidates, is required to be between 55 and 100 GeV. After this selection six data events remain, while 6.0 ± 0.8 SM background events are expected. The selection efficiency in this channel is $\sim 25\%$ for $M_{q^*} = 120$ GeV, increasing to 40% for $M_{q^*} = 260$ GeV.

In the search for $q^* \rightarrow qW \rightarrow q\mu\nu$, events with $P_T^{\rm miss} > 25$ GeV, one muon with $P_T^\mu > 10$ GeV and one jet with $P_T^{\rm jet} > 15$ GeV are selected. The muon and the jet must be detected in the polar angle ranges $5^\circ < \theta^e < 100^\circ$ and $5^\circ < \theta^\mu < 160^\circ$, respectively. To reduce the background contribution from W production, the P_T of the jet is required to be larger than 25 GeV in the polar angle range $\theta^{jet} < 60^\circ$. A W candidate is reconstructed from the combination of the four-vectors of the muon and neutrino candidates and its mass is required to be larger than 40 GeV. After this selection five data events remain, while 4.4 ± 0.7 SM background events are expected. The selection efficiency in this channel is $\sim 25\%$ for $M_{q^*} = 120$ GeV, increasing to 50% for $M_{q^*} = 260$ GeV.

5.4 qee and $q\mu\mu$ Resonance Searches

In the search for $q^* \rightarrow qZ \rightarrow qee$, events with two electrons and one jet of high transverse momenta are selected. The two electrons must be detected in the polar angle range $5^\circ < \theta^e < 100^\circ$ and have transverse momenta larger than 20 and 10 GeV, respectively. The jet must be detected in the polar angle range $5^\circ < \theta^{\rm jet} < 100^\circ$ and have a transverse momentum larger than 20 GeV. To reduce the background from QED Compton and NC DIS processes, each electron must be associated to a well measured track and be isolated from any other track by a minimum distance of $R > 0.5$. A Z candidate is reconstructed from the combination of the two electrons and its reconstructed mass is required be compatible with the nominal Z boson mass within 7 GeV. After this selection no data event remains, while 0.44 ± 0.08 SM background events are expected.

In the search for $q^* \rightarrow qZ \rightarrow q\mu\mu$, events with two muons and one jet of high transverse momenta are selected. The two muons must be detected in the polar angle range $5^\circ < \theta^\mu < 160^\circ$ and have transverse momenta larger than 15 and 10 GeV, respectively. The jet must be detected in the polar angle range $5^\circ < \theta^{\rm jet} < 100^\circ$ and have a transverse momentum larger than 20 GeV. A Z candidate is reconstructed from the combination of the two muons and its reconstructed mass is required to be larger than 50 GeV.

In both channels, the selection efficiency is $\sim 35\%$ for q^* with masses above 120 GeV.

5.5 Systematic Uncertainties

The following experimental systematic uncertainties are considered:

- The uncertainty on the electromagnetic energy scale varies between 0.7% and 2% depending on the polar angle. The polar angle measurement uncertainty is 3 mrad for electromagnetic clusters.
- The efficiency to identify photons is known with a precision of 10% for high P_T photons.
- The scale uncertainty on the transverse momentum of high P_T muons amounts to 2.5%. The uncertainty on the reconstruction of the muon polar angle is 3 mrad.
- The hadronic energy scale is known within 2%. The uncertainty on the jet polar angle determination is 10 mrad.
- The uncertainty on the trigger efficiency is 3%.
- The luminosity measurement has an uncertainty of 3%.

The effect of the above systematic uncertainties on the SM expectation and the signal efficiency is determined by varying the experimental quantities by ± 1 standard deviation in the MC samples and propagating these variations through the whole analysis chain.

Additional model systematic uncertainties are attributed to the SM background MC generators described in section 3. An error of 20% on the normalisation of NC DIS, CC DIS and photoproduction processes with at least two high P_T jets is considered to account for the uncertainty on higher order QCD corrections. The error on the elastic and quasi-elastic QED Compton cross sections is conservatively estimated to be 5%. The error on the inelastic QED Compton cross section is 10%. The errors attributed to lepton pair and W production are 3% and 15%, respectively. The total error on the SM background prediction is determined by adding the effects of all model and experimental systematic uncertainties in quadrature.

The theoretical uncertainty on the q^* production cross section is estimated to be 10%.

6 Interpretation

The event yields observed in all decay channels are in agreement with the corresponding SM expectations and are summarised in table 1. The SM predictions are dominated by photoproduction and NC DIS for the $q\gamma$ and $qq\bar{q}$ resonance searches and by W production for the $qe\nu$ and $q\mu\nu$ resonance searches. The distributions of the invariant mass of the data events are in agreement with those of the expected SM background as shown in figure 1. No data events are observed in channels corresponding to leptonic decays of the Z boson, in agreement with the low SM expectations.

Since no evidence for the production of excited quarks is observed, upper limits on the q^* production cross section and on the model parameters are derived as a function of the mass of the excited quark. Limits are presented at the 95% confidence level (CL) and are obtained from the mass spectra using a modified frequentist approach which takes statistical and systematic uncertainties into account [40].

The resulting limit on f/Λ after combination of all decay channels is displayed as a function of the q^* mass in figure 2, for $f_s = 0$ and the conventional assumption $f = +f'$. Considering the assumption $f/\Lambda = 1/M_{q^*}$ excited quarks with masses up to 259 GeV are excluded. The relative contributions of the q^* decay channels to the combined limit are shown in figure 2(a). These new results extend the previously published limits by H1 [2] and ZEUS [41] by a factor of two to five in f/Λ and constraints on q^* masses beyond the HERA kinematical limit are set. Excited quarks with masses below 500 GeV are excluded for coupling values $f/\Lambda > 0.05$.

7 Conclusion

Using the full $e^{\pm}p$ data sample collected by the H1 experiment at HERA with an integrated luminosity of 475 pb^{-1} a search for the production of excited electrons is performed. The excited quark decay channels $q^* \to q\gamma$, $q^* \to qZ$ and $q^* \to qW$ with subsequent hadronic or leptonic decays of the W and Z bosons are considered and no indication of a signal is found. Within gauge mediated models, an upper limit on the coupling f/Λ as a function of the excited quark mass is established for the specific relations $f = +f'$ and $f_s = 0$ between the couplings. Assuming $f = +f'$, $f_s = 0$ and $f/\Lambda = 1/M_{q^*}$ excited quarks with a mass lower than 259 GeV are excluded at 95% confidence level. The results presented in this paper extend previously excluded domains at HERA and LEP and are complementary to q^* searches performed at the Tevatron.

References

[1] H. Harari, Phys. Rept. **104** (1984) 159.

[2] C. Adloff *et al.* [H1 Collaboration], Eur. Phys. J. C **17** (2000) 567 [arXiv:hep-ex/0007035].

[3] F. D. Aaron *et al.* [H1 Collaboration], Phys. Lett. B **663** (2008) 382 [arXiv:0802.1858 [hep-ex]].

[4] F. D. Aaron *et al.* [H1 Collaboration], Accepted by Phys. Lett. B, arXiv:0805.4530 [hep-ex].

[5] K. Hagiwara, S. Komamiya and D. Zeppenfeld, Z. Phys. C **29** (1985) 115.

[6] U. Baur, M. Spira and P. M. Zerwas, Phys. Rev. D **42** (1990) 815.

[7] F. Boudjema, A. Djouadi and J. L. Kneur, Z. Phys. C **57** (1993) 425.

[8] S. J. Brodsky and S. D. Drell, Phys. Rev. D **22** (1980) 2236.

[9] F. M. Renard, Phys. Lett. B **116** (1982) 264.

[10] E. Boos *et al.* [CompHEP Collaboration], Nucl. Instrum. Meth. A **534** (2004) 250 [hep-ph/0403113];
A. Pukhov *et al.*, “CompHEP - a package for evaluation of Feynman diagrams and integration over multi-particle phase space”, hep-ph/9908288
(available at http://theory.sinp.msu.ru/comphep).

[11] T. Köhler, “Exotic Processes At Hera: The Event Generator Compos”, Proceedings of the Workshop “Physics at HERA”, eds. W. Buchmüller and G. Ingelman, DESY (1991), vol. 3, p. 1526.

[12] C. Berger and W. Wagner, Phys. Rept. **146** (1987) 1.

[13] J. Pumplin *et al.*, JHEP **0207** (2002) 012 [hep-ph/0201195].

[14] T. Sjöstrand *et al.*, PYTHIA version 6.1, Comput. Phys. Commun. **135** (2001) 238 [hep-ph/0010017].

[15] H. Jung, RAPGAP version 3.1, Comput. Phys. Commun. **86** (1995) 147.

[16] A. Kwiatkowski, H. Spiesberger and H. J. Möhring, Comput. Phys. Commun. **69** (1992) 155.

[17] G. A. Schuler and H. Spiesberger, DJANGOH version 1.4, “Django: The Interface for The Event Generators Heracles and Lepto”, Proceedings of the Workshop “Physics at HERA”, eds. W. Buchmüller and G. Ingelman, DESY (1991), vol. 3, p. 1419.

[18] L. Lönnblad, Comput. Phys. Commun. **71** (1992) 15.

[19] C. Adloff *et al.* [H1 Collaboration], Eur. Phys. J. C **25** (2002) 13 [hep-ex/0201006].

[20] A. Aktas *et al.* [H1 Collaboration], Phys. Lett. B **602** (2004) 14 [hep-ex/0408044].

[21] C. Berger and P. Kandel, “A New Generator For Wide Angle Bremsstrahlung,” Proceedings of the Workshop “Monte Carlo Generators for HERA Physics”, eds. A. T. Doyle, G. Grindhammer, G. Ingelman and H. Jung, DESY (1998).

[22] U. Baur, J. A. Vermaseren and D. Zeppenfeld, Nucl. Phys. B **375** (1992) 3.

[23] T. Abe, GRAPE-Dilepton version 1.1, Comput. Phys. Commun. **136** (2001) 126 [hep-ph/0012029].

[24] R. Brun, *et al.*, “Geant3,” CERN-DD/EE/84-1.

[25] I. Abt *et al.* [H1 Collaboration], Nucl. Instrum. Meth. A **386** (1997) 310;
I. Abt *et al.* [H1 Collaboration], Nucl. Instrum. Meth. A **386** (1997) 348.

[26] B. Andrieu *et al.* [H1 Calorimeter Group Collaboration], Nucl. Instrum. Meth. A **336** (1993) 460.

[27] B. Andrieu *et al.* [H1 Calorimeter Group Collaboration], Nucl. Instrum. Meth. A **350** (1994) 57.

[28] B. Andrieu *et al.* [H1 Calorimeter Group Collaboration], Nucl. Instrum. Meth. A **336** (1993) 499.

[29] R. D. Appuhn *et al.* [H1 SPACAL Group Collaboration], Nucl. Instrum. Meth. A **386** (1997) 397.

[30] C. Kleinwort [H1 Collaboration], "H1 alignment experience," *Prepared for 1st LHC Detection Alignment Workshop, Geneva, Switzerland, 4-6 Sep 2006*

[31] C. Adloff *et al.* [H1 Collaboration], Eur. Phys. J. C **30** (2003) 1 [hep-ex/0304003].

[32] V. Andreev *et al.* [H1 Collaboration], Phys. Lett. B **561** (2003) 241 [hep-ex/0301030].

[33] F. D. Aaron *et al.* [H1 Collaboration], Submitted to Phys. Lett. B, arXiv:0806.3987 [hep-ex].

[34] M. Peez, "Recherche de déviations au Modèle Standard dans les processus de grande énergie transverse sur le collisionneur électron - proton HERA", Ph.D. thesis, Université de Lyon (2003), DESY-THESIS-2003-023
(available at http://www-h1.desy.de/psfiles/theses/).

[35] B. Portheault, "Première mesure des sections efficaces de courant chargé et neutre avec le faisceau de positrons polarisé à HERA II et analyses QCD-électrofaibles", Ph.D. thesis, Université Paris XI (2005), LAL-05-05
(available at http://www-h1.desy.de/psfiles/theses/).

[36] S. D. Ellis and D. E. Soper, Phys. Rev. D **48** (1993) 3160 [hep-ph/9305266].

[37] S. Catani *et al.*, Nucl. Phys. B **406** (1993) 187.

[38] C. Adloff *et al.* [H1 Collaboration], Eur. Phys. J. C **13** (2000) 609 [hep-ex/9908059].

[39] A. Blondel and F. Jacquet, Proceedings of the Study of an ep Facility for Europe, ed. U. Amaldi, DESY 79/48 (1979) 391.

[40] T. Junk, Nucl. Instrum. Meth. A **434** (1999) 435 [hep-ex/9902006].

[41] S. Chekanov *et al.* [ZEUS Collaboration], Phys. Lett. B **549** (2002) 32 [hep-ex/0109018].

[42] P. Abreu *et al.* [DELPHI Collaboration], Eur. Phys. J. C **8** (1999) 41 [hep-ex/9811005].

Search for q^*, HERA I+II (475 pb^{-1}, preliminary)

Channel	Data	SM	Signal Efficiency [%]
$q^* \to q\gamma$	47	47 ± 7	35–45
$q^* \to qW/Z \to qq\bar{q}$	346	338 ± 137	5–60
$q^* \to qW \to qe\nu$	6	6.0 ± 0.8	25–40
$q^* \to qW \to q\mu\nu$	5	4.4 ± 0.7	25–50
$q^* \to qZ \to qee$	0	0.44 ± 0.08	35
$q^* \to qZ \to q\mu\mu$	0	0.87 ± 0.08	35

Table 1: Observed and predicted event yields for the studied q^* decay channels. The analysed data sample corresponds to an integrated luminosity of 475 pb^{-1}. The errors on the SM predictions include model and experimental systematic errors added in quadrature. Typical selection efficiencies for q^* masses ranging from 120 to 260 GeV are also indicated.

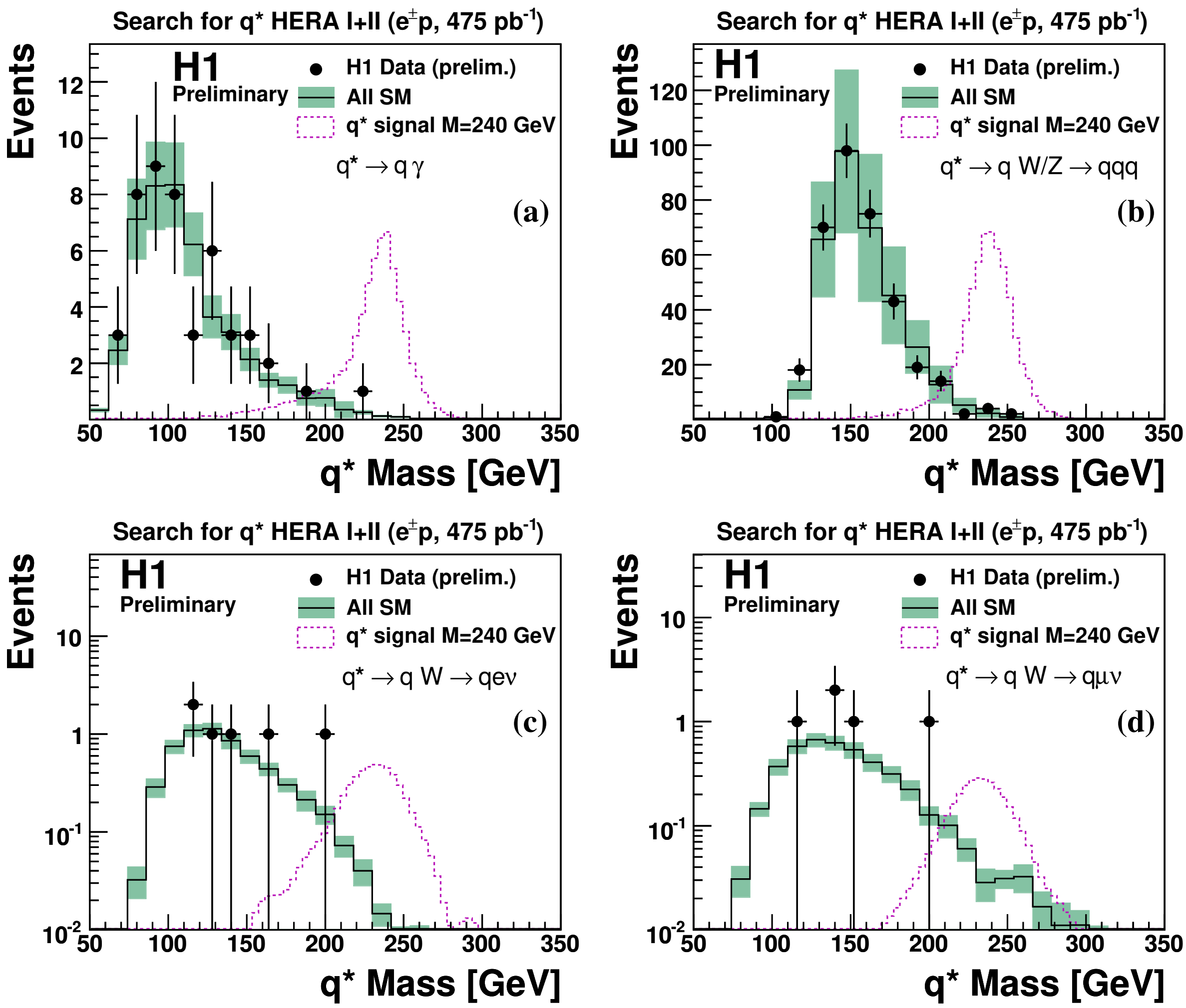

Figure 1: Invariant mass distribution of the q^* candidates in the $q^* \to q\gamma$ (a), $q^* \to qW/Z \to qq\bar{q}$ (b), $q^* \to qW \to qe\nu$ (c), and $q^* \to qW \to q\mu\nu$ (d) search channels. The points correspond to the observed data events and the histograms to the SM expectation after the final selections. The error bands on the SM prediction include model uncertainties and experimental systematic errors added in quadrature. The dashed line represents with an arbitrary normalisation the reconstructed mass distribution of q^* events with $M_{q^*} = 240$ GeV.

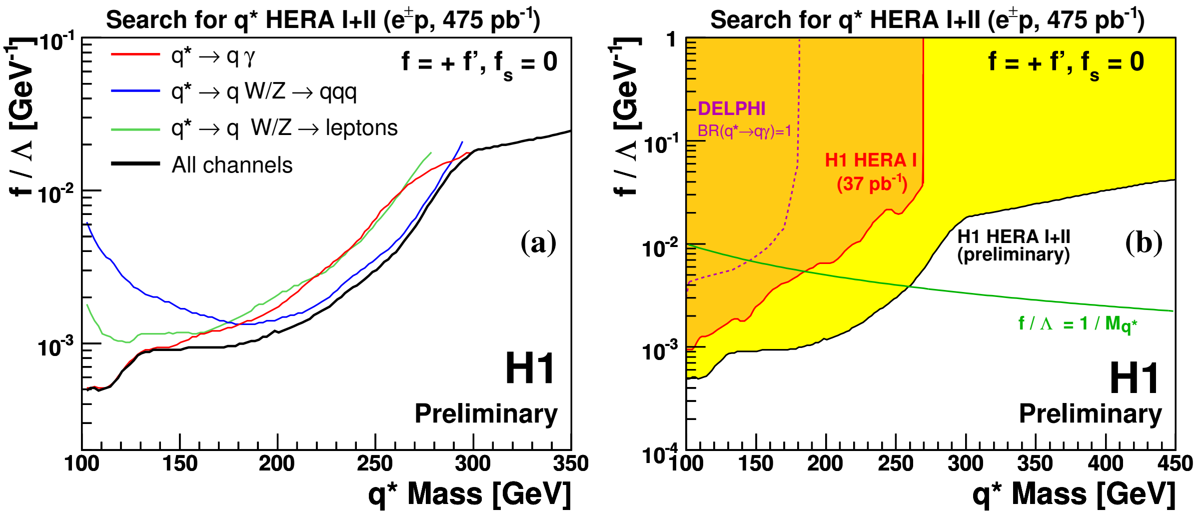

Figure 2: Exclusion limits at 95% CL on the coupling f/Λ as a function of the mass of the excited quark with the assumptions $f = +f'$ and $f_s = 0$. The separate contributions of the different q^* decay channels are presented in (a). Values of the couplings above the curves are excluded. The excluded domain based on all H1 $e^{\pm}p$ data is represented in (b) by the shaded area. It is compared to exclusion limit obtained at LEP by the DELPHI Collaboration [42] (dashed line), assuming tha the branching ratio of the $q^* \rightarrow q\gamma$ is equal to 1. The orange-dark area corresponds to the exclusion domain published by the H1 experiment [2] using HERA I data at $\sqrt{s} = 300$ GeV.